

Research Article

Chronostratigraphic Studies of the Ootun Area Revealing the Late Holocene Plume Volcanism of the Oldoinyo Lengai, Ngorongoro, Tanzania

Mohamed Zengo Makongoro ^{1,2}, Maheswara Rao Vegi ², Said Ali Hamad Vuai ²,
and Michael Mwita Msabi ³

¹Laboratory Directorate, Geological Survey of Tanzania, P. O. Box, 903 Dodoma, Tanzania

²Department of Chemistry, College of Natural and Mathematical Sciences, The University of Dodoma, P. O. Box, 259 Dodoma, Tanzania

³Department of Geology, College of Earth Sciences and Engineering, The University of Dodoma, P. O. Box, 259 Dodoma, Tanzania

Correspondence should be addressed to Maheswara Rao Vegi; vegi.rao@udom.ac.tz

Received 28 April 2022; Revised 6 August 2022; Accepted 18 August 2022; Published 5 September 2022

Academic Editor: Fan Yang

Copyright © 2022 Mohamed Zengo Makongoro et al. This is an open access article distributed under the Creative Commons Attribution License, which permits unrestricted use, distribution, and reproduction in any medium, provided the original work is properly cited.

Oldoinyo Lengai has been a subject of international attention for geoscientists because of its uniqueness. The mountain is the world's only active natrocarbonatite volcano whose recent activities are well documented. However, little is known about its eruptive history during the Holocene. One way of uncovering past volcanic activities is through chronostratigraphic studies. A rare stratigraphic sequence in the Ootun area containing buried tephra beds and paleosols is presented in this article. The beds suggest that the nearby active Oldoinyo Lengai volcano experienced the main plume volcanism during the late Holocene. This work presents the lithology of the area, estimated deposition period, and elemental and mineralogical compositions of strata, and establishing similarities between ash properties and information from previously reported chemistry and eruptions of the Oldoinyo Lengai volcano. Energy dispersive X-ray fluorescence, X-ray diffractometry, and accelerated mass spectrometry techniques were used for elemental, mineralogical, and radiocarbon dating analyses. A 1.3-m vertical soil profile revealed three major strata: topsoil, tephra bed, and paleosols. The paleosols are presumed to have been topsoil of the Ootun area during the Holocene. Subsurface tephra layers were found to contain similar properties to the volcanic material of the Oldoinyo Lengai. Based on the experimental findings and literature data, the study reports the occurrence of two major plume eruption events from the Oldoinyo Lengai, which happened around the minimum (oldest) age of 490 ± 10 BC and 771 AD. This work is essentially important in demonstrating the relevance of the region's tephra chronostratigraphic studies by revealing the prospect of collecting additional scientific data on past geological processes and paleoenvironmental conditions of northern Tanzania.

1. Introduction

For thousands of years, explosive volcanism of Oldoinyo Lengai blanketed a surface area of about 1200 km^2 with pyroclastic deposits that scatter across the central and western Ngorongoro and settle on the landscapes (Figure 1), thereby modifying the chemistry of the soil and possibly veg-

etation cover [1, 2]. Materials from Oldoinyo Lengai, mainly pyroclastic deposits, have been reported to have settled down as far as 100 km west of the mountain covering the areas from Ootun to Olduvai Gorge (Figure 1) and some parts of eastern Serengeti plains [1]. As a result, the soil geochemistry of the region has primarily been influenced by the eruptive history of the Oldoinyo Lengai. The primary drive

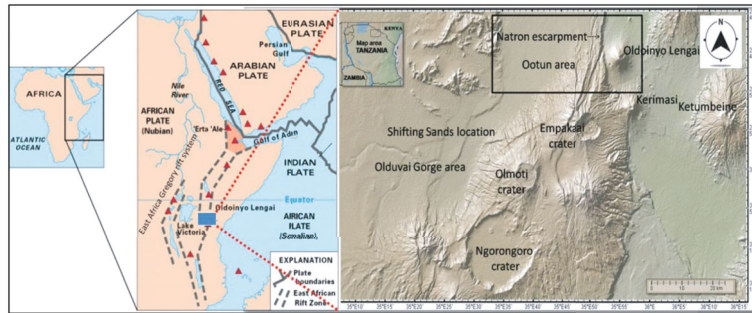


FIGURE 1: A map of Eastern branch of the East African Rift system (the Gregory Rift System) showing the study site (a rectangle) and associated areas in the eastern, central, and western parts of Ngorongoro. The East African Rift System, commonly known as the Afro-Arabian Rift Valley, is one of the largest rift systems on Earth's surface, stretching from Jordan in southwestern Asia south across eastern Africa to Mozambique. The system is approximately 6,400-km long and 48 to 64-km wide on average.

for ash transfer is associated with violent Plinian eruptions and the strength of the current and historical East-West winds that help take coarse to fine material with them [2].

A general term for airborne pyroclastic materials is tephra [3]. These are large quantities of particles produced by explosive volcanic eruptions, and once they are in the atmosphere, they combine with the surrounding air to form an eruption column or volcanic plume [4]. Tephra materials are divided into four categories based on their size, coarse ash, fine ash, lapilli, and volcanic bombs or blocks [5].

Tephra fallout may be syn-eruption or inter-eruption. The former is the time period during an eruption and immediately thereafter when activity ceases, in which there is a considerable sediment delivery. The latter marks the point at which the geomorphic system has stabilized. The syn-eruption deposits are basically instantly deposited sediments that were created at rapid rates. They typically exhibit little lithologic variety and are abundant in pyroclastic materials with sand- and ash-size grains. On the other hand, inter-eruption volcanoclastic deposits often exhibit significant lithological diversity, and gravel-bedload facies are quite prevalent [6].

Tephra fallout is frequently used in research, and its significance is mainly restricted to proximal and medial distances from the source [5]. Its applications include, among other things, the reconstruction of past eruptive events to constrain important eruption parameters and tephrochronology studies [7–9]. Besides tephrochronology, volcano geology is a powerful tool to follow [6, 9, 10]. Chronostratigraphy is well known for its power to uncover stratigraphic sequences by digging pits of varying depths and assigning radiometric or non-radiometric ages in layers [11, 12].

Paleosols have been used by researchers in chronostratigraphic studies when the tephra bed is unqualified for the requirement of radiometric tests. They are ancient soils that formed on ancient landscapes [13]. Most paleosols in the sedimentary record have been covered by lava, volcanic ash, landslides, flood debris, or landslides [13]. While certain paleosols are mostly found on the earth's surface, they are no longer forming in the same manner as they did in the past under different climatic and vegetative environments [13]. The carbon-14 age of the paleosol immediately below the

tephra bed represents the minimum deposition age of the tephra [14]. The carbon-14 dates of the paleosols in chronostratigraphic studies have been reported elsewhere [15–18].

In this study, chrono-stratigraphy was used in the Ootun area where the established soil profile was made and the carbon-14 of the paleosol [1, 19], Energy Dispersive X-ray fluorescence (XRF) and X-ray diffractometry (XRD) of subsurface tephra beds were studied. The carbon-14 age of the paleosol immediately below the subsurface tephra bed represents the minimum (oldest) age of deposition of the subsurface tephra bed, and the chemical and mineralogical facies [20] were described and used to correlate the source of the subsurface tephra bed. Volcanic rocks make great chronometers. Consequently, volcanic rocks with a large areal dispersion can offer superior chrono-correlation horizons [6]. This information helps address the timing of explosive volcanism and source volcano and is essential to address important information that allows the understanding of past volcanic events and the history of the Tanzanian Gregory Rift volcanoes.

2. Geological Settings

The study area includes the Ootun and Oldoinyo Lengai areas located at Lake Natron-Engaruka Monogenic Volcanic fields (LNE-MVF) that host about 150 scoria cones [21]. There is currently not enough data to establish a refined or high-resolution chronology of volcanism, though they are estimated to range between Pleistocene and Holocene [22, 23]. The area is within Northern Tanzania's East African Rift zone (Figure 1), which experiences active tectonic plate movements associated with the volcanic activities of the mountains in the region [24]. The study area is subdivided into two parts; the Lake Natron Basin, which hosts Oldoinyo Lengai, and the Ootun area on the West (Figures 1–3). The Ootun area hosts several tephra piles of sizes ranging from 1 to 5 m high, up to 40 m wide, and is generally flat with short savannah grasslands (Figure 4). The two parts are separated by the Natron escarpment (the Gregory rift scarp), the Western part being relatively higher in altitude (Figure 2).

Oldoinyo Lengai was first shown on a map dated 14th March 1855, compiled by two missionaries, Erhardt and

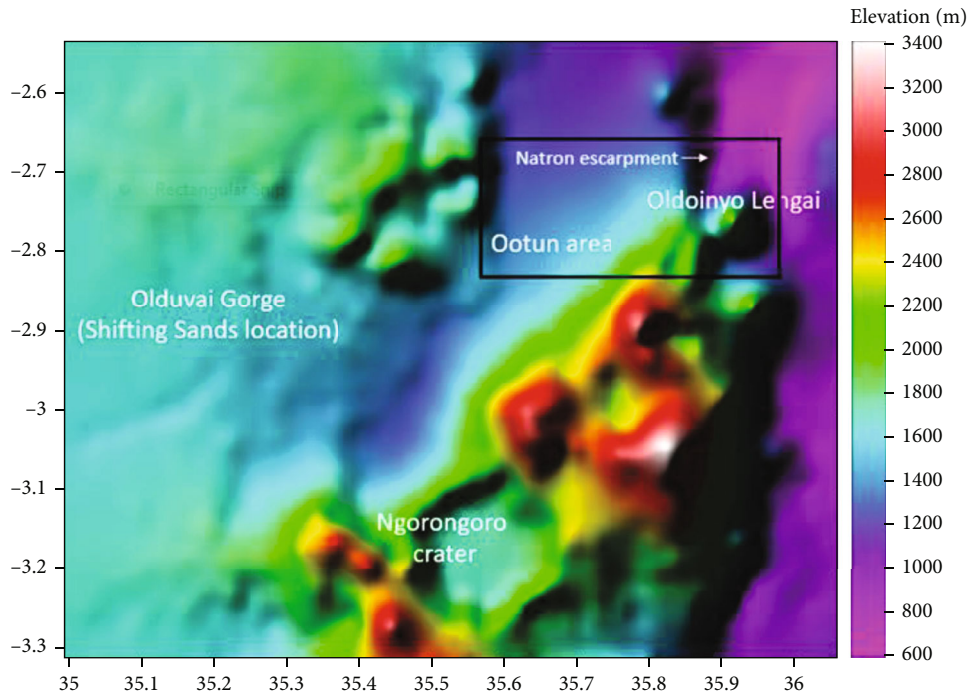


FIGURE 2: A map of part of the Northern Tanzanian sector of the Gregory rift produced from the Shuttle Radar Topography Mission (SRTM) digital elevation dataset using Surfer software version 16. The map shows the altitude relationships of different areas associated with the study site (in a rectangle). The map covers all of the northern parts of the Ngorongoro Conservation Area.

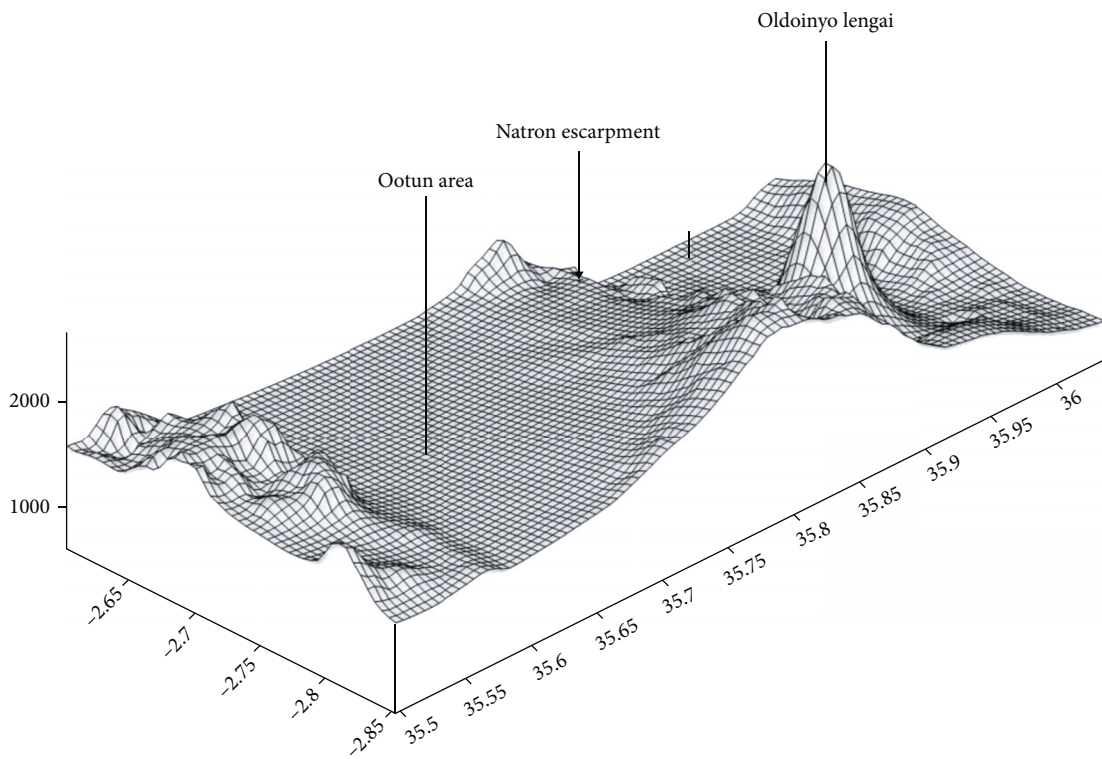


FIGURE 3: A 3D model of the study site (shown in a rectangle in Figures 1 and 2) was generated from the SRTM digital elevation dataset using Surfer software version 16. The model presents a typical topographic view that defines different morphological patterns of the study site.



FIGURE 4: A photo of the Ootun area depicting the landscape featuring several tephra piles presumed to be ash fallouts (Tephra piles) from Oldoinyo Lengai. Their shapes suggest they were once in motion due to the influence of wind, as regular fallouts could not create such a well-placed pattern but as a result of post-deposition reworking ($2^{\circ}46'44''\text{S}$ $35^{\circ}36'16''\text{E}$). Insert: A closer view of the tephra pile surface.

Rebmann, based at Kisaludini near Mombasa [25]. However, the first account of the age estimations and timings of volcanic activities came from stratigraphic investigations at Olduvai Gorge, about 75 km west of Oldoinyo Lengai [1]. Olduvai Gorge is one of the most important sites in the world as one of the sources of archeological information regarding human evolution [26–28]. Stratigraphic studies at Olduvai Gorge uncovered the widely known stratigraphic sequence that contains four beds, namely, Masek, Ndutu, Naisiusiu, and Namorod [1]. Of particular interest to this article are the Ndutu, Naisiusiu, and Namorod beds which were reported to contain ash layers presumably originating from Oldoinyo Lengai [1]. The $^{40}\text{Ar}/^{39}\text{Ar}$ dating of the Ndutu layers estimates the age of the material to be 450 to 220 ka [29], while that of Naisiusiu beds has 22 to 15 ka ^{14}C ages obtained from pedogenic calcium carbonate. Both Ndutu and Naisiusiu beds had been correlated to the yellow tuff of Unit I of the Oldoinyo Lengai cone [23, 25]. It has further been reported that the volcanic activity of the Oldoinyo Lengai continued 15 ka years ago [2]. The radiocarbon age of Naisiusiu and a terrestrial gastropod fossil under the ash layer at Namorod bed is dated at 1,250 years BP. Hay [1] supports this assumption. The Namorod bed is correlated to the black tuff of unit III of the Oldoinyo Lengai cone [25]. The account of the appearance of Oldoinyo Lengai ash at Olduvai Gorge is essentially significant in this study as it portrays the scope of material disperse and potential future boundaries for tephra stratigraphic studies in the region.

Generally, $^{40}\text{Ar}/^{39}\text{Ar}$, $^{40}\text{K}/^{40}\text{Ar}$, and ^{14}C radiometric techniques have been the key techniques for past studies in addressing the age or eruptive history of the Oldoinyo Lengai volcano and surroundings [1, 2, 30, 31]. From these techniques, researchers came up with different age estimations from samples collected around the area. It is estimated that from 800,000 to 600,000 years ago, the Oldoinyo Lengai volcanic activities were well in progress [2]. A phonolite rock taken “near Oldoinyo Lengai,” for example, was reported to have an age of around 150 ka years of $^{40}\text{K}/^{40}\text{Ar}$ radiomet-

ric studies, and no other details were provided [2, 30]. On the other hand, radiocarbon analysis was reported from soil samples aged about 3500 ^{14}C BP underlying ash on the eastern part of the mountain [1]. Different radiocarbon ages of about 2,050 to 1,300 years were also reported from soil layers below the ash deposits 16 km north of the volcano [1, 19]. The most recent radiocarbon ages were those reported by Keller et al. [31] on the fallout material at the 1200 meters altitude on the volcano’s eastern flank, aged about 3,000 to 2,500 BP. A list of radiometric ages of Oldoinyo Lengai is presented in Table 1.

Oldoinyo Lengai is one of the youngest stratovolcanos in East Africa, whose volcanism was well followed up during the past century [25, 32]. For recent activities of Oldoinyo Lengai, Dawson et al. [25] is the most recommended reference. Two main types of activities by the volcano have been reported. These are lava flows and ash-emitting, mostly Plinian-type explosive eruptions. The lava flow was witnessed from 1904 to the end of 1916 [25]. Ash eruptions were recorded in 1917, 1926, and 1940 followed by lava extrusion from 1958 to 1966. The Ash eruption phase reappeared from 1966 to 1967 and 1983. In 1983 another ash eruption was recorded [25]. Later on, lava flow with light ash eruption episodes from 2007 to 2008, 2010, and the latest 2013 were also registered [25]. While it is essential to have accurate data on the volcano behavior, including the frequency and magnitude of both ash eruption and lava extrusions throughout the history of the volcano whenever possible, there is currently no accurate and consistent information on the volcano, making it difficult to predict future volcanic activities for hazards and environmental management purposes.

3. Materials and Methods

3.1. Study Site. The sampling site was selected based on the topography, distance from Oldoinyo Lengai, and history of the wind direction. The Ootun area is about 35 km west of Oldoinyo Lengai (Figures 5 and 6). It is a lowland ideal for accommodating and preserving sediments. The western and southern parts of the Ootun area are highlands of varying heights (1700–3400 m). During a clear sky, Oldoinyo Lengai is visible from the Ootun area which is about 35 km. The site is covered with piles of ash material presumed to be old tephra material (Figure 4). Currently, the wind direction is East to West making it ideal for ash material to land in the area during eruption periods of the Oldoinyo Lengai.

3.2. Sampling. A total of four points located 500 m apart were selected for sampling in the Ootun area. Given that the subsurface tephra bed covers a large area, a 1.5 km total sampling distance (500 m x 3) (Figure 6) ensures that the stratigraphic depth and number of layers were uniform and fairly looked almost identical. Additionally, the accuracy of the results is improved by a large number of samples and sampling points. Pits were dug to about 1.3 to 1.5 m to expose all layers above the paleosols (Figure 7) [12]. Each pit is considered as a profile (1, 2, 3, and 4 in Figure 6).

TABLE 1: Radiometric ages around the Oldoinyo Lengai.

| Material | Method | Reported ages | Source |
|--------------------------------|------------------------------------|----------------------------|--------|
| Tuff | K/Ar | 600 ka | [1] |
| Whole rock | K/Ar | 0.15 ± 0.02 ma | [33] |
| Organic matter | Carbon-14 | 3,000 and 2,500 years B.P. | [31] |
| Calcium carbonate-bearing soil | Carbon-14 | 2,050 and 1,300 years B.P. | [19] |
| Calcareous soil deposits | Carbon-14 | 3,500 ± 100 14C years B.P. | [1] |
| Tuff | K/Ar | 1.37 ma | [34] |
| Alkali feldspar | ⁴⁰ Ar/ ³⁹ Ar | 338 ka | [2] |
| Phlogopite | ⁴⁰ Ar/ ³⁹ Ar | 353 ka | [2] |
| Phlogopite | ⁴⁰ Ar/ ³⁹ Ar | 460 ka | [2] |
| Phlogopite | ⁴⁰ Ar/ ³⁹ Ar | 763 ka | [2] |

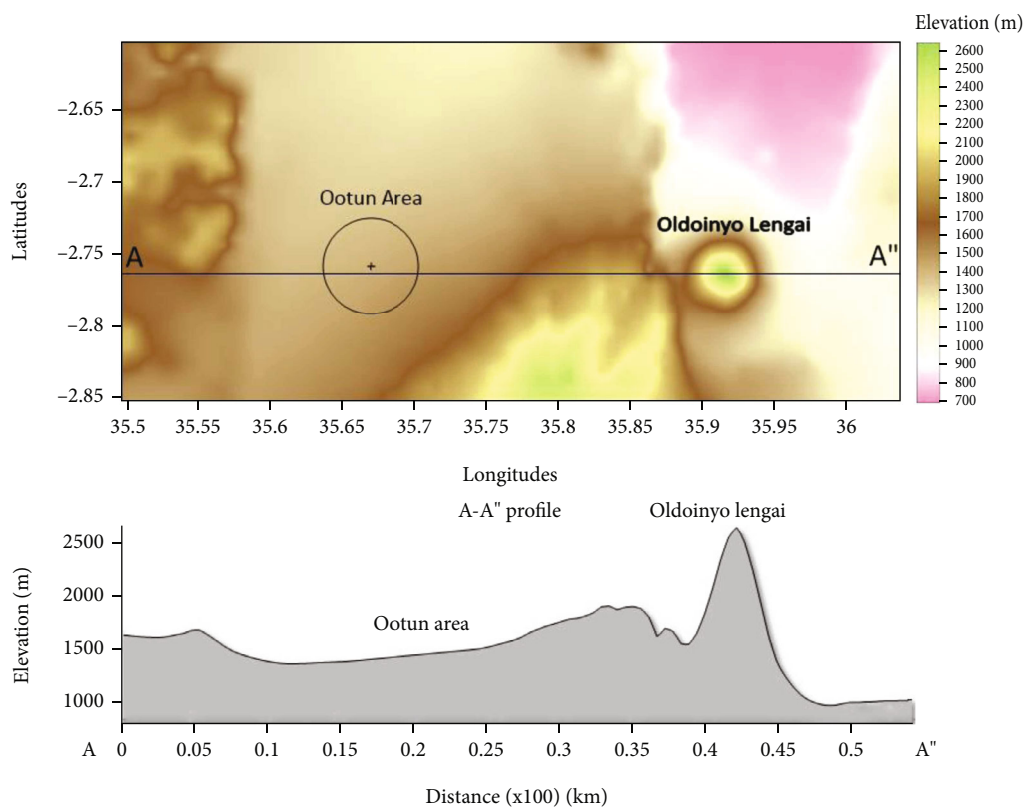


FIGURE 5: Top: A map of the study site generated from the SRTM digital elevation dataset using Surfer software version 16. The map shows topographic and distance relationships between the Ootun area where tephra piles and subsurface tephra beds are located and Oldoinyo Lengai, a suspected tephra source. Bottom: A cross-section of points A-A'' from a topographic map showing side view elevations of the study area.

The paleosols' thicknesses were not fully recovered as it was the interest of this study to reveal layers above the paleosols. A spade (for tephra pile material) and a clean metal pipe 30-cm long and 5-cm diameter (for the lower compacted layers) were used for sampling. A total of six samples were collected from each of the four pits, where two samples were taken from the layers of Ootun sand piles (OTS), buried ash (BASH), and organic buried ash (OBA) (Table 2). OTS sampling was done at two points, namely, the surface (S) and 60 cm deep in the tephra pile (B). The arrows in

Figure 7(b) indicate the color transition from brownish to dark brown due to infiltration of soil solution and oxic-anoxic transition from top to bottom. The bottom dash line looks compact on the top. The core sampling position of the paleosols (OBA) was also selected to ensure the top part was engaged for better ash radiocarbon interpretation (2°46'44"S 35°36'16"E). Furthermore, a total of eight samples of ash material (OLA series) were collected from four different locations (two from each) at the foot of Oldoinyo Lengai, which is situated about 35 km East of the Ootun area

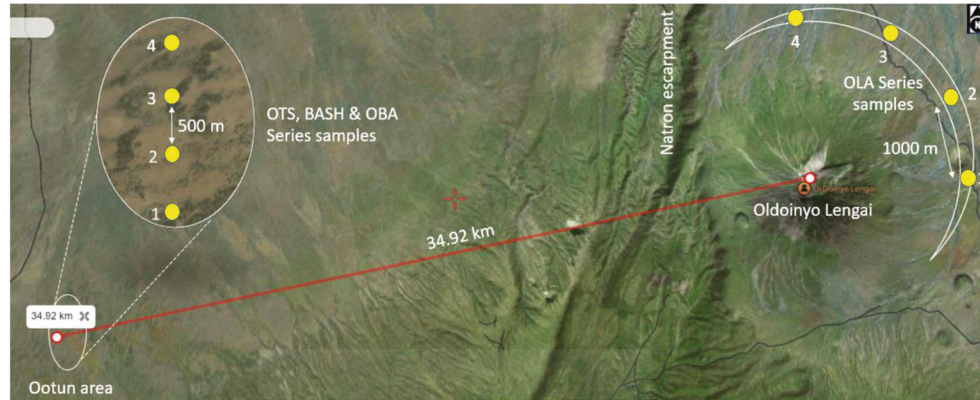


FIGURE 6: A map showing the sample locations (1, 2, 3, and 4) in relation to geographical features.

(Figures 6 and 7(d)). As a whole, 32 samples were collected (Table 2).

3.3. Lithostratigraphic and Mineralogical Studies. The colors and texture of the materials in the soil profile were described in relation to strata arrangement. The strata characteristics were described considering the law of superposition, where the youngest strata are always placed at the top, assuming no disturbances to the system occurred [35].

Two samples, namely, BASH and OBA, from subsurface tephra and paleosol strata, respectively, from the second profile (Figure 6 and 7(c)), were analyzed by XRD machine model BTX II to acquire spectra and mineralogical compositions for characterization and correlation purposes. The analysis was performed at the Department of Geology, University of Dar es Salaam.

3.4. Age Determination of Tephra Layers. Age determination for the subsurface tephra layer was determined indirectly by analyzing ^{14}C of the underlying paleosols strata as described in Keller et al. [16]. Tephra layers were not suitable for direct determination of age using ^{14}C , $^{40}\text{Ar}/^{39}\text{Ar}$, $^{40}\text{K}/^{40}\text{Ar}$, or luminescence techniques as they contained insufficient carbon content which then will not work over 30 ka (for ^{14}C). The material showed signs of weathering making them unable to retain argon gas, hence unfit for Ar-Ar and K-Ar radiometric methods [36–38]. Furthermore, K-Ar is a fairly challenging and time-consuming task and is unlikely to work below 50 ka. Insufficient quartz crystals in tephra layers could make the material unable to trap sufficient electrons in quartz structures, rendering them unsuitable for luminescence dating techniques [37].

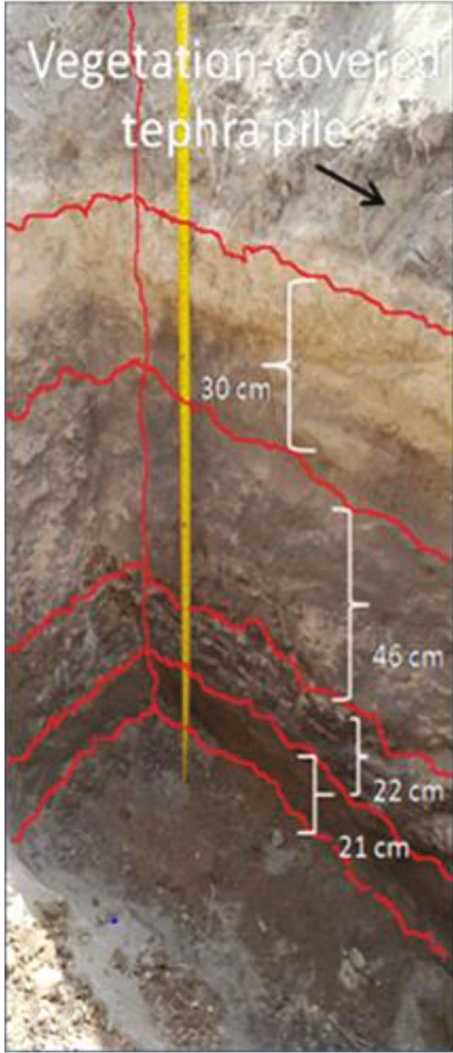
Paleosol samples were first visually inspected for size, homogeneity, debris, inclusions, clasts, grain size, organic constituents, and potential contaminants. It was then dispersed in de-ionized water, homogenized through stirring and sonication, and then sieved through a $180\ \mu\text{m}$ sieve. The material sieved was used for the analysis. The material was bathed in 1.25 N HCl at 90°C for a minimum of 1.5 hours to ensure removal of carbonates, followed by serial de-ionized water rinses at 70°C until neutrality was reached. Any debris or micro-rootlets were discarded during these rinses. After drying in an oven at 100°C for 12–24 hours,

HCl was applied to representative subsamples under the microscope to validate the absence of carbonates. A microscopic examination was performed to assess its characteristics and determine the appropriate subsamples for accelerated mass spectrometer (AMS) dating. The AMS measurement was done using NEC 250 keV Single Stage AMS on a humic acid fraction of the sample, converted to graphite form. Calibration of radiocarbon age to calendar years was done according to Ramsey [39] by applying the SHCAL13 database [40]. Conversion of ^{14}C ages and sigma were rounded to ten years as per the 1977 International Radiocarbon Conference and consistent with past laboratory analytic radiocarbon dates. The analysis was performed at the Beta Analytic Testing Laboratory at 4985 S.W. 74th Court, Miami, Florida 33155 (USA).

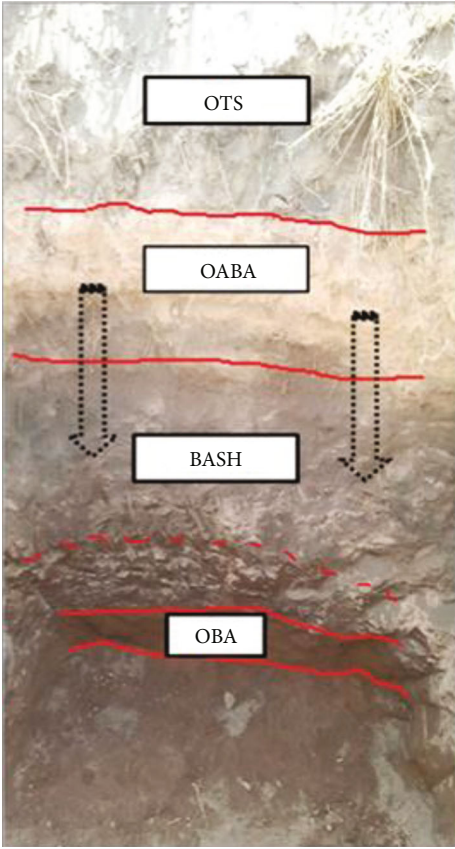
3.5. Determination of Chemical Composition. All tephra samples from the Ootun area and Oldoinyo Lengai ash were examined by removing debris before being dried at 105°C for two hours and homogenized. Representative samples of about 200 g were pulverized to $75\ \mu\text{m}$ before determining chemical composition by XRF machine as described in Lowe [9]. A Niton XRF machine Model XL3t was used for elemental determination of the samples. The machine was equipped with gold and silver anodes and a high-performance semiconductor detector. The maximum scan was at 50 kV and $40\ \mu\text{A}$ for all samples. To improve the sensitivity for light elements, an external helium system was connected to the machine during analyses. The determination was done in laboratory benchtop settings. Certified reference standard DC73026 from China National Analysis Centre for Iron and Steel (Beijing) was used for calibration. The analyses were performed at the Geological Survey of Tanzania (GST) Laboratory.

4. Results

4.1. Lithostratigraphic and Mineralogical Studies. The minimum depth of the vertical soil profile was about 1.3 m, of which three distinct strata were identified. A 30 cm brownish soil layer (OABA) followed by a second blackish tephra layer (BASH) at about 30 to 68 cm below the surface was revealed from the top. The overall soil profile compactness increases



(a)



(b)

FIGURE 7: Continued.

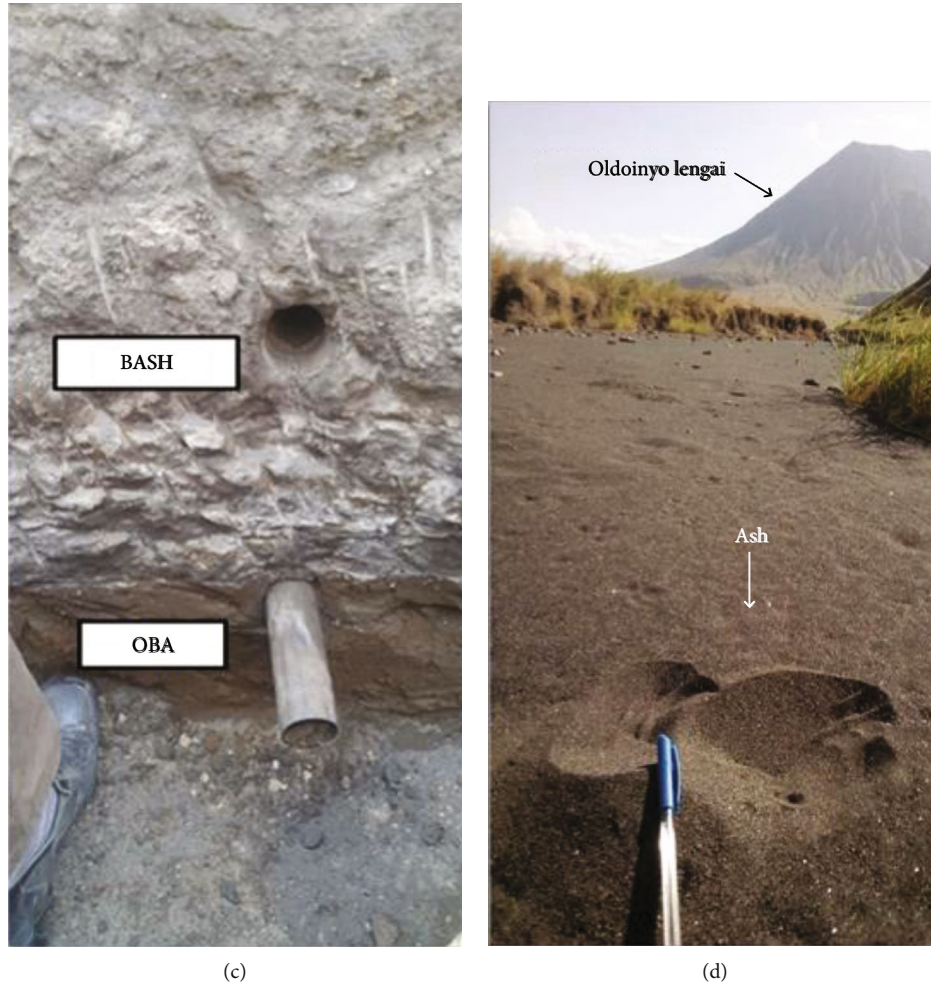


FIGURE 7: The soil stratigraphy in the Ootun area. (a) Stratigraphic distances in centimeters (b) A profile showing the tephra pile (OTS), topsoil (organic after buried ash, OABA), subsurface lower and upper tephra bed (BASH), and paleosol (OBA); (c) core sampling of the last two layers, BASH and OBA, and (d) one of the ash sample locations at Oldoinyo Lengai ($2^{\circ}45'31''\text{S } 35^{\circ}54'51''\text{E}$).

TABLE 2: Sampling budget.

| Serial no. | Sample type | Sample name | Location | Sample no. | Mass (g) |
|------------|---------------------|-------------|-----------------|------------|----------|
| 1 | Ash | OTS series | Ootun area | 8 | 1000 |
| 2 | Subsurface tephra | BASH series | Ootun area | 8 | 1000 |
| 3 | Subsurface Paleosol | OBA series | Ootun area | 8 | 1000 |
| 4 | Ash | OLA series | Oldoinyo Lengai | 8 | 1000 |
| | | | Total samples | 32 | |

with depth until the last paleosol layer, sharply decreasing. The blackish tephra layer was the most compacted and was the layer of interest in which further mineralogical studies were carried out using an XRD machine. The profile color changes from brownish at the top to darkish at the bottom (Figure 7).

According to XRD analysis, the blackish tephra layer (BASH) mineral assemblage is mainly nepheline (41.5%), muscovite (26.9%), potassium feldspar (microcline) (19.2%), and small amounts of aegirine (3.5%), pargasite (4.7%), and siderite (3.1%) (Figure 8). The last blackish layer

was characterized by very fine particles of clay presumed to be a paleosol (OBA). The XRD scan results for the sample from these strata consist predominantly of nepheline (23.4%), calcite (17.5%), illite (15.6%), muscovite (14.4%), and biotite (9.7%), as indicated in the spectra in Figure 8.

4.2. Age Determination of Tephra Layers. The radiometric age of the subsurface tephra layer was determined indirectly by estimating the age of the underlying paleosols. The sample's age from the topmost part of the paleosol has been used to define the timing of the tephra deposition. The



FIGURE 8: XRD results for samples BASH and OBA.

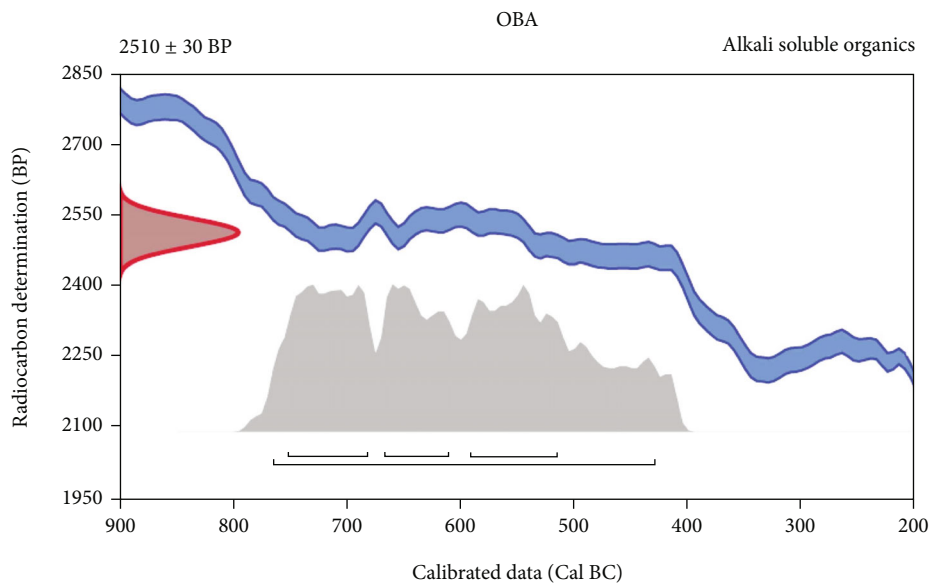


FIGURE 9: A radiocarbon calibration curve for paleosol sample (OBA) from OxCal software. The y-axis shows the radiocarbon ages expressed in years “before present (BP),” while the x-axis shows corresponding calendar years. The blue-colored graph is the calibrated line based on known values of ¹⁴C ages, including tree rings. The graph is presented in two lines for one standard deviation. The distribution curve on the y-axis represents the ¹⁴C concentrations in the sample, while the gray curve on the x-axis shows the corresponding probabilities of ages for the sample.

TABLE 3: Summary of the results for ^{14}C age of the paleosol samples determined by AMS. Calibration of radiocarbon age to calendar years was done using OxCal software.

| Laboratory number | Sample name | Probability (%) | Uncalibrated radiocarbon age | Calibrated radiocarbon measurement | Conventional radiocarbon age |
|-------------------|-------------|-----------------|------------------------------|------------------------------------|------------------------------|
| Beta-570767 | OBA | 95.4 | 2715-2379 cal BP | 766-430 cal BC | 2510 \pm 30 BP |
| | | 24.9 | 2702-2631 cal BP | 753-682 cal BC | |
| | | 24.3 | 2542-2465 cal BP | 593-516 cal BC | |
| | | 18.9 | 2618-2560 cal BP | 669-611 cal BC | |
| Beta-570767a | OBA(a) | 95.5 | 2715-2379 cal BP | 766-436 cal BC | 2510 \pm 30 BP |
| | | 24.6 | 2702-2631 cal BP | 753-502 cal BC | |
| | | 24.6 | 2542-2565 cal BP | 593-616 cal BC | |
| | | 18.2 | 2618-2553 cal BP | 669-511 cal BC | |
| Beta-570767b | OBA(b) | 95.7 | 2715-2888 cal BP | 766-477 cal BC | 2510 \pm 30 BP |
| | | 24.0 | 2702-2630 cal BP | 753-671 cal BC | |
| | | 24.3 | 2542-2465 cal BP | 593-516 cal BC | |
| | | 18.7 | 2618-2551 cal BP | 669-642 cal BC | |
| Beta-570767c | OBA(c) | 95.6 | 2715-2398 cal BP | 766-453 cal BC | 2510 \pm 30 BP |
| | | 24.4 | 2702-2601 cal BP | 753-672 cal BC | |
| | | 24.1 | 2542-2461 cal BP | 593-512 cal BC | |
| | | 19.1 | 2618-2572 cal BP | 669-633 cal BC | |

radiocarbon age calibration to calendar years adopted a higher probability density range method and was calculated using OxCal software (Figure 9), and the results are summarized in Table 3.

4.3. Chemical Composition. The chemical composition of samples from tephra piles (OTS series) was found to have concentrations of silicon dioxide ranging from 43.71 to 48.88%, aluminum oxide ranging from 9.14 to 10.74%, iron oxide ranging from 6.17 to 9.13%, and calcium oxide ranging from 10.07 to 13.75%. Other oxides such as potassium and titanium show slightly lower values of 1.14% to 2.11% and 2.24 to 2.99%, respectively. Lower values of some trace elements have also been detected (Table 4). Slightly elevated values of major oxide concentrations in samples taken from the top of the tephra pile (OTS ‘‘S’’ series) are observed in SiO_2 and Na_2O . On the other hand, Fe_2O_3 , CaO , and MgO values for the same samples are relatively low compared to the samples taken 60 cm deep from the same tephra piles.

Generally, there is an agreement on the chemical composition of samples from subsurface tephra (BASH) and Oldoinyo Lengai ash (OLA). They fall under the same range for all major oxides except for MgO . The elevated MgO data in BASH (underground tephra bed) samples was unknown, despite the fact that sampling, sample preparation, and analysis precautions were all the same. However, because Oldoinyo Lengai is a stratovolcano and its ash composition can change over time (between basalt and rhyolite) [2], it is suggested that during the formation of the tephra bed, the composition of MgO was different (Table 4).

5. Discussion

Tephra’s dispersion and deposition over the western side of Gregory Rift volcanos is not new. An account of the tephra layers traced to Gregory Rift volcanoes at the Olduvai Gorge is of high value to this study [1]. During the study, a site survey witnessed several tephra piles across the western part of Oldoinyo Lengai to the Olduvai Gorge area (Figure 2). However, the tephra piles were modified into barchans and reduced by wind action as they move westwards for thousands of years [41], and only a few have remained, including the barchan, famed ‘‘Shifting Sand’’ (which is a tourist attraction) approximately 2.5 km from Olduvai Gorge (Figures 2 and 10). These tephra piles and surface ash fall-outs may have resulted from several past depositions at varying times and in varying amounts. An excellent example of such deposits resulted from a recent eruption of Oldoinyo Lengai in 2007-2008 reported by Sherrold et al. [2], where the eruption caused massive ash fallout on the western part of Oldoinyo Lengai.

While volcanic eruptions typically last a short time in a volcano’s overall history, the volume of loose pyroclastic product, when coupled with aeolian processes, can cause continuous and prolonged reworking of volcanic products. These wind-driven processes have a considerable impact on geomorphology and prolong the impact of eruptions on the ecosystem communities nearby [43].

The Ootun sand dunes are characterized by vegetation (vegetative sand dunes) (Figure 4), while those from the Olduvai Gorge have been constantly moving westwards (migrating sand dunes) (Figure 10) by the wind action, but they all have a common volcanic origin. They are black

TABLE 4: Major oxides and some trace element composition of samples from tephra pile (OTS), subsurface tephra (BASH), and Oldoinyo Lengai ash (OLA).

| Sample ID | SiO ₂ % | Al ₂ O ₃ % | Fe ₂ O ₃ % | CaO % | Na ₂ O % | K ₂ O % | TiO ₂ % | MgO % | SO ₃ % | P ₂ O ₅ % | V Ppm | Mn Ppm | Ni Ppm | Zn Ppm | As Ppm | W Ppm | Cu Ppm | Ba Ppm | Y Ppm | Zr Ppm |
|-----------|-----------------------|-------------------------------------|-------------------------------------|----------|------------------------|-----------------------|-----------------------|----------|----------------------|------------------------------------|----------|-----------|-----------|-----------|-----------|----------|-----------|-----------|----------|-----------|
| OTS 1S | 48.12 | 10.72 | 6.87 | 10.48 | 8.88 | 1.19 | 2.24 | 0.84 | 0.24 | 0.49 | 149 | 2351 | 116 | 205 | 49 | 1.08 | 105 | 1086 | 34 | 609 |
| OTS 1B | 43.91 | 9.89 | 9.11 | 13.75 | 6.41 | 2.02 | 2.62 | 2.05 | 0.41 | 0.42 | 121 | 2298 | 124 | 195 | 45 | 1.22 | 120 | 968 | 45 | 564 |
| OTS 2S | 48.88 | 9.69 | 6.17 | 10.07 | 8.11 | 1.91 | 2.92 | 1.14 | 0.46 | 0.52 | 145 | 2248 | 136 | 145 | 48 | 1.45 | 142 | 956 | 45 | 582 |
| OTS 2B | 43.71 | 9.14 | 8.49 | 13.42 | 5.45 | 2.11 | 2.47 | 2.41 | 0.56 | 0.54 | 162 | 2298 | 156 | 168 | 67 | 1.65 | 163 | 987 | 41 | 612 |
| OTS 3S | 47.41 | 9.45 | 6.83 | 10.41 | 8.63 | 2.04 | 2.47 | 1.01 | 0.47 | 0.57 | 145 | 2314 | 122 | 157 | 59 | 1.35 | 125 | 1021 | 46 | 632 |
| OTS 3B | 45.01 | 10.74 | 9.13 | 13.14 | 5.14 | 1.14 | 2.79 | 2.02 | 0.56 | 0.41 | 124 | 2365 | 141 | 175 | 58 | 1.24 | 111 | 1045 | 42 | 624 |
| OTS 4S | 48.43 | 9.73 | 6.76 | 10.11 | 9.19 | 1.91 | 2.99 | 1.78 | 0.78 | 0.44 | 155 | 2395 | 178 | 164 | 47 | 1.45 | 123 | 1033 | 47 | 598 |
| OTS 4B | 43.89 | 9.27 | 9.48 | 12.79 | 6.75 | 1.43 | 2.38 | 2.47 | 0.72 | 0.57 | 133 | 2244 | 154 | 146 | 64 | 1.32 | 124 | 1092 | 48 | 574 |
| BASH 1A | 45.76 | 6.32 | 7.88 | 14.98 | 6.22 | 2.91 | 1.45 | 5.41 | 0.34 | 0.16 | 152 | 1985 | 127 | 169 | 45 | 1.78 | 137 | 858 | 37 | 537 |
| BASH 1B | 43.31 | 6.45 | 9.56 | 12.51 | 6.42 | 3.12 | 1.55 | 6.02 | 0.35 | 0.22 | 166 | 2014 | 166 | 199 | 45 | 2.11 | 199 | 955 | 47 | 658 |
| BASH 2A | 42.42 | 6.33 | 8.47 | 15.48 | 4.77 | 3.48 | 1.99 | 7.61 | 0.39 | 0.32 | 147 | 2014 | 145 | 201 | 12 | 2.32 | 154 | 965 | 36 | 655 |
| BASH 2B | 43.12 | 7.16 | 9.03 | 13.12 | 5.86 | 3.65 | 1.14 | 8.24 | 0.54 | 0.23 | 122 | 2035 | 124 | 205 | 14 | 2.54 | 148 | 845 | 95 | 622 |
| BASH 3A | 43.17 | 7.16 | 9.11 | 14.13 | 4.11 | 2.45 | 1.35 | 8.11 | 0.75 | 0.24 | 189 | 2058 | 165 | 168 | 86 | 2.10 | 198 | 985 | 47 | 654 |
| BASH 3B | 43.04 | 6.34 | 8.12 | 12.81 | 5.92 | 2.89 | 2.01 | 8.64 | 0.56 | 0.30 | 147 | 2021 | 147 | 167 | 49 | 2.05 | 178 | 852 | 48 | 678 |
| BASH 4A | 43.14 | 6.14 | 10.03 | 13.34 | 5.13 | 3.11 | 2.22 | 8.58 | 0.65 | 0.25 | 149 | 2025 | 164 | 189 | 19 | 2.09 | 188 | 847 | 48 | 548 |
| BASH 4B | 43.16 | 6.75 | 8.38 | 14.42 | 5.89 | 3.02 | 1.99 | 8.54 | 0.45 | 0.25 | 146 | 1969 | 124 | 177 | 75 | 2.55 | 149 | 655 | 25 | 695 |
| OLA 1A | 42.11 | 7.11 | 11.14 | 14.88 | 4.12 | 1.11 | 2.94 | 3.23 | 0.49 | 0.69 | 126 | 2911 | 28 | 289 | 46 | 1.19 | 105 | 1700 | 59 | 679 |
| OLA 1B | 41.91 | 6.83 | 10.63 | 15.09 | 3.93 | 1.14 | 3.11 | 3.23 | 0.58 | 0.78 | 153 | 2916 | 22 | 279 | 41 | 1.14 | 95 | 1717 | 47 | 817 |
| OLA 2A | 42.11 | 6.96 | 10.62 | 14.41 | 3.82 | 1.07 | 3.21 | 3.23 | 0.41 | 0.65 | 147 | 2844 | 24 | 289 | 31 | 1.19 | 87 | 1817 | 68 | 645 |
| OLA 2B | 41.43 | 7.25 | 10.48 | 14.95 | 5.01 | 1.06 | 3.24 | 3.23 | 0.43 | 0.75 | 185 | 2719 | 19 | 297 | 39 | 1.28 | 112 | 1845 | 59 | 712 |
| OLA 3A | 42.75 | 7.11 | 10.72 | 15.15 | 3.71 | 1.05 | 2.81 | 3.23 | 0.39 | 0.74 | 165 | 2990 | 35 | 212 | 29 | 1.27 | 91 | 1847 | 49 | 634 |
| OLA 3B | 41.38 | 7.02 | 10.76 | 15.08 | 4.47 | 1.14 | 3.09 | 3.23 | 0.44 | 0.64 | 147 | 2849 | 31 | 254 | 49 | 1.24 | 102 | 1791 | 47 | 711 |
| OLA 4A | 41.22 | 7.06 | 10.78 | 15.07 | 4.16 | 0.89 | 3.45 | 3.23 | 0.49 | 0.75 | 195 | 2844 | 29 | 271 | 55 | 1.23 | 117 | 1844 | 52 | 694 |
| OLA 4B | 42.49 | 7.12 | 9.96 | 15.10 | 4.12 | 0.98 | 3.26 | 3.23 | 0.54 | 0.65 | 158 | 2838 | 22 | 249 | 35 | 1.11 | 87 | 1746 | 55 | 621 |



FIGURE 10: The barchan famed “Shifting Sand” near Olduvai Gorge area ($2^{\circ}56'32''\text{S}$ $35^{\circ}18'42''\text{E}$). The Shifting Sand is a tourist attraction for many decades (source [42]).

and magnetic in nature because they contain a more than 80% augite mineral [41] which imparts the material with magnetic properties [44]. While the black magnetic sand dunes are very uncommon, they are difficult to compare (chemically and geographically) with other desert and semi-arid sand dunes in Africa (e.g., Namibia, Egypt, Mali, and Morocco), and the Arabian Peninsula (e.g., Saudi Arabia, Yemen, and Oman) and with dunes in different continents (e.g., Italy, Australia, and the USA). This is because the former originates from a unique volcanic eruption, while the latter is not. However, there are a few examples of magnetic ash dune fields which are similar to those found in the Ngorongoro area. The Great Sand Dunes National Park which is found in Rio Grande rift, Colorado, USA, is one of them [45].

Most of the cones from the Gregory Rift are stratovolcanoes, and their ash fallouts vary from time to time [2, 46]. The fallouts from different eruptions may physically mix up. Examining the chemistry and petrology of surface ash fallouts to ascertain volcanic eruption periods and correlation studies becomes complicated because their chemical and petrographic results are difficult to interpret but worth indicative data. Due to this fact, the study has concentrated on the undisturbed tephra layers buried underground.

A stratigraphic overview of the soil profile in the Ootun area provides valuable information about the eruptive history of the neighboring volcanoes. The volume and space of the tephra piles occupy in the Ootun area before and after the deposition provides evidence of how tall and fast upthrust the volcanic plume worked. While the dune-shape and southeast direction of the piles suggest that they were once in motion, their current state is almost stationary and inactive (stabilized dunes). This is evident by the growth of vegetation on them.

Moreover, tephra layers as one of the stratigraphic units in the Ootun area constitute a piece of key evidence that at a particular time in history, violent volcanic eruptions associated with plumes occurred in the region. According to petrographic studies of the subsurface tephra layer, nearly three quotas of the material consist of primarily nepheline and muscovite minerals. At the same time, the rest is a feldspar with siderite aegirine and pargasite as minor mineral phases. Several studies have reported the dominant mineral phases in the Gregory east volcanos to be nephelinitic with mica-

related minerals such as biotite, muscovite, olivine, and various feldspars [47–54]. The observed similarities of rock-forming minerals in the subsurface tephra of the Ootun area and those found from Gregory Rift volcanic eruptions are striking and informative for tracing the source volcano of Ootun subsurface tephra.

The thickness of the subsurface tephra layer provides a clue as to the distance between the source volcano and these materials. A tephra layer of more than 30-cm thick in the Ootun area rules out the likelihood of originating from one or more of the small volcanic cones in the Gregory Rift region of northern Tanzania. The large volcanic cone with a history of eruption is responsible for erupting these materials. The Ootun area is 30 to 45 km east of the Gregory Rift volcanic cones, where these materials are presumed to have originated. Perhaps the most important question is: Which volcano was the source of them? A historical account that addresses volcanism in the Gregory Rift eastern part is of valuable contribution to answering this question. In addition, the deposition time of these layers may offer information about the eruption periods of the possible source volcano.

The Oldoinyo Lengai volcano is the only active peak in the region that has continued its activities to varying magnitudes since 600 ka [1, 25]. Kerimasi mountain, located 12 km southeast of Oldoinyo Lengai, was formed nearly the same time as Oldoinyo Lengai. But according to $^{40}\text{K}/^{40}\text{Ar}$ radiometric dating studies of the mountain rocks, Kerimasi had been reported to cease its volcanic activities about 400 ka years ago [55, 56]. Results from ^{14}C analysis of the paleosols in the soil profile at the Ootun area indirectly estimate the minimum (oldest) age of deposition of the tephra layers of about 2510 ± 30 cal BP. During this period, more than three eruption activities of the Oldoinyo Lengai had been reported [1, 19]. Of far greater importance is the one reported by Keller et al. [31], which was the most recent mention of the radiometric dating of the Oldoinyo Lengai volcano. It reports the eruption of the Oldoinyo Lengai that occurred between 3000 and 2500 cal BP using organic samples underlying tephra fallout on its eastern flanks. According to the radiocarbon age of the tephra layer at the Ootun area of about 2510 ± 30 cal BP revealed in this study, the deposition time of tephra materials agrees with the Oldoinyo Lengai eruption reported by Keller et al. [31]. The radiocarbon ages reported in this study are considered reliable and accurate as the ^{14}C AMS method has adopted the most advanced probabilistic calibration approach by *OxCal* software [39]. The dating method used humic acid fraction for graphite formation to generate carbon dioxide gas injected in the AMS. While contamination of humic acid fraction and the fresh organic matter remains imminent in soil dating using the radiocarbon method [57], making the material appear younger than it is, the dated soil layer was close to one meter below the surface and under the most compacted tephra layer, making it almost impossible for contamination of any kind to occur (Figure 7). The paleosol samples were taken right below the line separating the paleosols from the subsurface tephra layer (Figure 7(c)) in order to ensure proper interpretation of the carbon-14 results. The carbon-

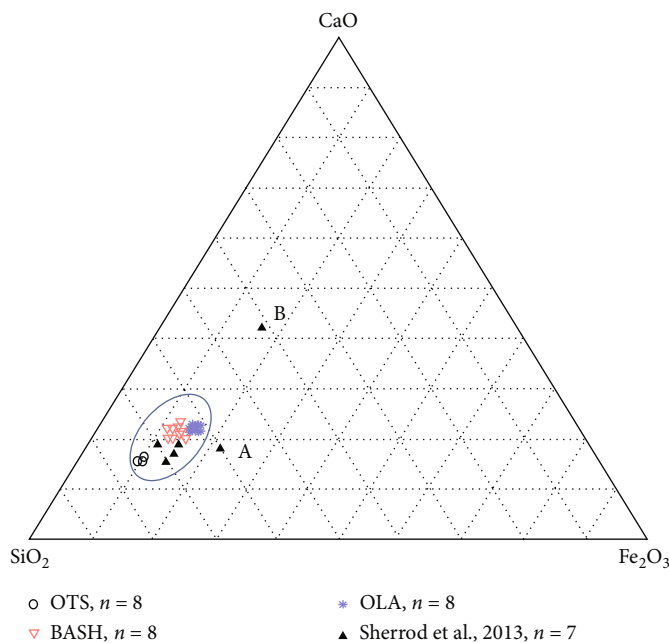


FIGURE 11: A CaO-SiO₂-Fe₂O₃-ternary system for Ootun samples (OTS and BASH) and Oldoinyo Lengai Ash (OLA). The plot includes five samples from Oldoinyo Lengai's western flanks and two other samples ((a) and (b) in the plot) from other Gregory Rift volcanic cones reported by Sherrod et al. [2].

14 results of the paleosol samples give the minimum age of the ash fallouts, which leads to tephra formation almost in the same period of time.

The elemental composition of tephra pile samples from the Ootun area (Table 4) demonstrates differences in composition between surface samples and samples taken 60-cm deep. Elevated values of SiO₂ and Na₂O and lower concentrations of Fe₂O₃, CaO, and MgO for surface samples are noticeable. This may be due to differences in concentrations of ash fallouts at different times.

Despite difficulties in interpreting chemical data of ash fallout due to ash mixing from separate eruptions, the chemical analyses of tephra piles at the Ootun area (Figure 4) and Oldoinyo Lengai ash (Figure 7(d)) demonstrate a rational agreement on elemental compositions (Table 4 and Figure 11). Geochemical fingerprinting has widely been used to trace sources of ash elsewhere [58–60]; however, a multidisciplinary approach greatly increases the likelihood of ash originality. A CaO-SiO₂-Fe₂O₃-ternary system (Figure 11) that includes the results of the elemental composition of five samples of tephra fallouts from the western flanks of the Oldoinyo Lengai [2] shows a positive correlation to chemical data from subsurface tephra samples of the Ootun area, suggesting that they may be sharing the source volcano.

Based on the topographic layout of the Ootun area, Oldoinyo Lengai, field stratigraphy, and laboratory findings, the study hypothesizes the occurrence of two major tephra fallouts from two major plume volcanic events of Oldoinyo Lengai; the first occurred around the minimum (oldest) age of about 2510 ± 30 BP (490 ± 10 BC) that lead to BASH tephra and another eruption after several unspecified years later, probably around 1,250 years BP (771 AD) for initial tephra deposition (OTS) on top (Figure 7). The later erup-

tion may be the one that led to the previously mentioned Namorod depositions at Olduvai Gorge, which was also reported by ¹⁴C dates of soil layers below the ash deposits 16km north of the Oldoinyo Lengai volcano [1]. The later occurrence is evident due to tephra piles on the surface with slightly different compositions from the subsurface tephra. Moreover, the two tephra depositions (i.e., tephra piles and subsurface tephra beds) are separated by a 30+ cm thick topsoil that the sedimentation process had later formed from the surrounding highlands. This process may have taken several hundred years after the subsurface tephra deposition event.

Verifying the surface tephra piles' age on the Ootun area's surface was difficult. This is because they were probably a product of a mixture of an undefined number of past ash fallouts from different volcanic eruptions which happened at different periods. The entire piles represent reworked ash accumulated in various wind conditions over a longer time. Their dune shapes underpin the hypothesis that they were once in motion, thereby facilitating the mixing of ash fallouts from different periods. Moreover, predicting the age of these tephra piles for indicative age through the underlying topsoil was also incredibly doubtful. This is because determining the age of soil using the radiocarbon method is challenging for topsoil due to the seasonal addition of new organic material from plants [61]. Moreover, the apparent mobility of the tephra piles during the distant past emanated from wind action precludes the concept of using topsoil as an indirect method of ascertaining their tentative depositional age.

6. Conclusions

The chronostratigraphic study of the Ootun area revealed a rare stratigraphic sequence containing buried tephra beds

and paleosols. According to radiocarbon dating, the buried tephra beds are estimated to have been deposited at a minimum (oldest) age of about 2510 ± 30 cal BP (490 ± 10 BC). Mineralogical and chemical compositions of ash material from the region suggest that the ash material originates from the major plume volcanism of Oldoinyo Lengai. The study also suggests that the second major plume volcanism of the Oldoinyo Lengai happened several hundred years later, perhaps around the minimum (oldest) age of about 1,250 years BP (771 AD). The later eruption is suggested to have generated massive ash fallouts that produced tephra piles at the Ootun area and perhaps that of the Namorod beds of the Olduvai Gorge [1]. Verifying the age of tephra piles at Ootun was difficult due to the possible mixing up of ash fallouts of different eruptive periods. Chemical analyses showed compositional differences in ash material from other periods reported by previous studies.

This study demonstrates the relevance of the region's tephra chronostratigraphic studies by revealing the prospect of collecting additional scientific data on past geological processes and paleoenvironmental conditions of northern Tanzania. To collect more data for reconstructing the region's past, more time-based eruption studies of the Oldoinyo Lengai are recommended to estimate eruption volumes and timings with a high degree of certainty.

Data Availability

All the data used to support the findings of this study is included in the article.

Conflicts of Interest

The authors declare that there is no conflict of interest with respect to the research, authorship, and/or publication of this article.

Acknowledgments

The authors recognize the valuable contribution of the Ngorongoro Conservation Area Authority (NCAA) in Tanzania for the tireless support they provided during fieldwork in the study area. The authors also appreciate the cooperation provided by Dr Charles Messo of the Geology Department, University of Dar es Salaam for his contribution to petrographic studies. Finally, the authors recognize the contribution of the staff of the Geological Survey of Tanzania Laboratory during the experimental work. This research was conducted as a part of PH. D program at The University of Dodoma. This is self-sponsored by the PH. D candidate (first author) under the supervision of the co-authors.

References

- [1] R. L. Hay, *Geology of the Olduvai Gorge: a study of sedimentation in a semiarid basin*, vol. 203, University of California Press, Berkeley, 1976.
- [2] D. R. Sherrod, M. M. Magitita, and S. Kwelwa, *Geologic map of Oldoinyo Lengai (Oldoinyo Lengai) and surroundings, Arusha region, United Republic of Tanzania*, vol. 65, U.S. geological survey Open-File Report 2013-1306, 2013, pamphlet.
- [3] S. Thorarinsson, "Greetings from Iceland," *Physical Geography*, vol. 63, no. 3-4, pp. 109-118, 1981.
- [4] A. Folch, "A review of tephra transport and dispersal models: evolution, current status, and future perspectives," *Journal of Volcanology and Geothermal Research*, vol. 235-236, pp. 96-115, 2012.
- [5] T. M. Wilson, C. Stewart, V. Sword-Daniels et al., "Volcanic ash impacts on critical infrastructure," *Physics and Chemistry of the Earth, Parts A / B / C*, vol. 45, pp. 5-23, 2011.
- [6] K. Németh and J. Palmer, "Geological mapping of volcanic terrains: discussion on concepts, facies models, scales, and resolutions from New Zealand perspective," *Journal of Volcanology and Geothermal Research*, vol. 385, pp. 27-45, 2019.
- [7] V. C. Smith, R. Isaia, and N. J. G. Pearce, "Tephrostratigraphy and glass compositions of post-15 kyr Campi Flegrei eruptions: implications for eruption history and chronostratigraphic markers," *Quaternary Science Reviews*, vol. 30, no. 25-26, pp. 3638-3660, 2011.
- [8] L. J. Connor and C. B. Connor, *Inversion is the key to dispersion: understanding eruption dynamics by inverting tephra fallout*, H. M. Mader, S. G. Coles, C. B. Connor, and L. J. Connor, Eds., *Statistics in volcanology: special publications of IAVCEI*, 1. Geological Society, London, 2006.
- [9] D. J. Lowe, "Tephrochronology and its application: a review," *Quaternary Geochronology*, vol. 6, no. 2, pp. 107-153, 2011.
- [10] J. Martí, G. GropPELLI, and A. Brum da Silveira, "Volcanic stratigraphy: a review," *Journal of Volcanology and Geothermal Research*, vol. 357, pp. 68-91, 2018.
- [11] O. Arnalds, "The influence of volcanic tephra (Ash) on ecosystems," *Advances in Agronomy*, vol. 121, pp. 331-380, 2013.
- [12] F. Zehetner, M. H. Gerzabek, J. Shellnutt et al., "Linking rock age and soil cover across four islands on the Galapagos archipelago," *Journal of South American Earth Sciences*, vol. 99, article 102500, 2020.
- [13] G. J. Retallack, *Paleosols*, *Reference Module in Earth Systems and Environmental Sciences*, Springer, 2014.
- [14] M. Okuno, T. Nakamura, H. Moriwaki, and T. Kobayashi, "AMS radiocarbon dating of the Sakurajima tephra group, Southern Kyushu, Japan," *Nuclear Instruments and Methods in Physics Research*, vol. 123, no. 1-4, pp. 470-474, 1997.
- [15] H. Kamata and T. Kobayashi, "The eruptive rate and history of Kuju volcano in Japan during the past 15, 000 years," *Journal of Volcanology and Geothermal Research*, vol. 76, no. 1-2, pp. 163-171, 1997.
- [16] O. Mitsuru and N. Toshio, "Radiocarbon dating of tephra layers: recent progress in Japan," *Quaternary International*, vol. 105, no. 1, pp. 49-56, 2003.
- [17] M. Okuno, "Tephrochronology and radiocarbon chronology in Japan," *The Quaternary Research (Daiyonki-Kenkyu)*, vol. 40, no. 6, pp. 461-470, 2001.
- [18] M. Ikuo, "Eruption age of Aso volcano, Komezuka," *J-STAGE top/Volcano*, vol. 55, no. 5, 2010.
- [19] R. L. Hay, "Holocene carbonatite-nephelinite tephra deposits of Oldoinyo Lengai, Tanzania," *Journal of Volcanology and Geothermal Research*, vol. 37, no. 1, pp. 77-91, 1989.
- [20] G. J. Orton, *Facies Models in Volcanic Terrains: Time's Arrow versus Time's Cycle*, Sedimentary Facies Analysis, A tribute to the research and teaching of Harold G. Reading, International Association of Sedimentologists Special Publications, 1988.

- [21] H. B. Mattsson and B. A. Tripoli, "Depositional characteristics and volcanic landforms in the Lake Natron-Engaruka monogenetic field, northern Tanzania," *Journal of Volcanology and Geothermal Research*, vol. 203, no. 1-2, pp. 23-34, 2011.
- [22] J. B. Dawson and D. G. Powell, "The Natron-Engaruka explosion crater area, northern Tanzania," *Bulletin of Volcanology*, vol. 33, no. 3, pp. 791-817, 1969.
- [23] J. B. Dawson, *The Gregory Rift Valley and Neogene-Recent Volcanoes of Northern Tanzania*, vol. 33, no. 1, 2008, Geological Society of London, London, Bath, 2008.
- [24] V. A. Meshili and J. H. Kwon, "Crustal movement at Oldoinyo Lengai based on GPS measurements," *Journal of the Korean Society of Surveying, Geodesy, Photogrammetry and Cartography*, vol. 38, no. 5, pp. 401-406, 2020.
- [25] J. B. Dawson, J. Keller, and C. Nyamweru, "Historic and recent eruptive activity of Oldoinyo Lengai," in *Carbonatite Volcanism*, K. Bell and J. Keller, Eds., vol. 4, Springer, Berlin, Heidelberg, 1995.
- [26] L. S. Leakey and M. D. Leakey, "Recent discoveries of fossil hominids in Tanganyika : at Olduvai and Near Lake Natron," *Nature*, vol. 202, no. 4927, pp. 5-7, 1964.
- [27] I. de la Torre, R. Mora, M. Dominguez-Rodrigo, L. de Luque, and L. Alcalá, "The Oldowan industry of Peninj and its bearing on the reconstruction of the technological skills of lower Pleistocene hominids," *Journal of Human Evolution*, vol. 44, no. 2, pp. 203-224, 2003.
- [28] E. M. De Tapia, I. D. Rubio, J. G. Castro, E. Solleiro, and S. Sedov, "Radiocarbon dates from soil profiles in the Teotihuacán valley, Mexico: indicators of geomorphological processes," *Radiocarbon*, vol. 47, no. 1, pp. 159-175, 2005.
- [29] P. C. Manega, *Geochronology, geochemistry, and isotopic study of the Plio-Pleistocene hominid sites and the Ngorongoro volcanic highland in northern Tanzania [PhD Thesis]*, University of Colorado, 1993.
- [30] A. Foster, C. Ebinger, E. Mbede, and D. Rex, "Tectonic development of the northern Tanzanian sector of the East African Rift System," *Journal of the Geological Society of London*, vol. 154, no. 4, pp. 689-700, 1997.
- [31] J. Keller, A. N. Zaitsev, and D. Wiedenmann, "Primary magmas at Oldoinyo Lengai: the role of olivine melilitites," *Lithos*, vol. 91, no. 1-4, pp. 150-172, 2006.
- [32] H. B. Mattsson and E. Reusser, "Mineralogical and geochemical characterization of ashes from an early phase of the explosive September 2007 eruption of Oldoinyo Lengai (Tanzania)," *Journal of African Earth Sciences*, vol. 58, no. 5, pp. 752-763, 2010.
- [33] G. P. Bagdasaryan, V. I. Gerasimovskiy, A. I. Polyakov, R. K. Gukasyan, and V. I. Vernadskiy, "Age of volcanic rocks in the rift zones of East Africa," *Geochemistry International*, vol. 10, pp. 66-71, 1973.
- [34] R. M. Macintyre, J. G. Mitchell, and J. B. Dawson, "Age of fault movements in Tanzanian sector of East African rift system," *Nature*, vol. 247, no. 5440, pp. 354-356, 1974.
- [35] E. C. Harris, "The laws of archaeological stratigraphy," *World Archaeology*, vol. 11, no. 1, pp. 111-117, 1979.
- [36] I. McDougall and T. M. Harrison, *Geochronology and thermochronology by the $^{40}\text{Ar}/^{39}\text{Ar}$ method*, Oxford University Press, Oxford, 1999.
- [37] M. Walker, *Quaternary dating methods*, John Wiley & Sons Ltd, The Atrium, Southern Gate, Chichester, Sussex PO19 8SQ, England, 2005.
- [38] M. J. Aitken, *Science-Based Dating in Archaeology*, Longman, London, 1990.
- [39] C. B. Ramsey, "Bayesian analysis of radiocarbon dates," *Radiocarbon*, vol. 51, no. 1, pp. 337-360, 2009.
- [40] A. G. Hogg, Q. Hua, P. G. Blackwell et al., "SHCal13 southern hemisphere calibration, 0-50,000 years cal BP," *Radiocarbon*, vol. 55, no. 4, pp. 1889-1903, 2013.
- [41] D. P. Kafumu, "The geochemical compositions and origin of sand dunes in the Olduvai Gorge-Eastern Serengeti plains, Northern Tanzania," *Tanzania Journal of Science*, vol. 46, no. 2, pp. 241-253, 2020.
- [42] F. Perelli, "Unusual places," 2017, (<https://unusualplaces.org/olduvai-gorge-the-shifting-sand-dunes/>) accessed on 24.07.2022.
- [43] L. Dominguez, C. Bonadonna, P. Forte et al., "Aeolian remobilisation of the 2011-Cordón Caulle tephra-fallout deposit: example of an important process in the life cycle of volcanic ash," *Frontiers in Earth Science*, vol. 7, p. 343, 2020.
- [44] A. Sigamony, "Magnetic properties of augite," *Proceedings of the Indian National Science Academy*, vol. 20, no. 5, pp. 261-265, 1945.
- [45] B. J. Drenth, V. J. S. Grauch, C. A. Ruleman, and J. A. Schenk, "Geophysical expression of buried range-front embayment structure: great sand dunes National Park, Rio Grande rift," *Geosphere*, vol. 13, no. 3, pp. 974-990, 2017.
- [46] J. B. Dawson, "Peralkaline Nephelinite-Natrocarnatite relationships at Oldoinyo Lengai, Tanzania," *Journal of Petrology*, vol. 39, no. 11-12, pp. 2077-2094, 1998.
- [47] A. N. Zaitsev, C. T. Williams, S. N. Britvin et al., "Kerimasite, $\text{Ca}_3\text{Zr}_2(\text{Fe}_{23}+\text{Si})\text{O}_{12}$, a new garnet from carbonatites of Kerimasi volcano and surrounding explosion craters, northern Tanzania," *Mineralogical Magazine*, vol. 74, no. 5, pp. 803-820, 2010.
- [48] T. D. Peterson, "Petrology and genesis of natrocarnatite," *Contributions to Mineralogy and Petrology*, vol. 105, no. 2, pp. 143-155, 1990.
- [49] A. N. Zaitsev, J. Keller, J. Spratt, T. E. Jeffries, and V. V. Sharygin, "Chemical composition of nyerereite and gregoryite from natrocarnatites of Oldoinyo Lengai volcano, Tanzania," *Geology of Ore Deposits*, vol. 51, no. 7, pp. 608-616, 2009.
- [50] E. P. Reguir, A. R. Chakhmouradian, M. N. Halden, P. Yang, and A. N. Zaitsev, "Early magmatic and reaction-induced trends in magnetite from the carbonatites of Kerimasi, Tanzania," *The Canadian Mineralogist*, vol. 46, no. 4, pp. 879-900, 2008.
- [51] J. Keller and M. Krafft, "Effusive natrocarnatite activity of Oldoinyo Lengai, June 1988," *Bulletin of Volcanology*, vol. 52, no. 8, pp. 629-645, 1990.
- [52] A. A. Church, *The petrology of the Kerimasi carbonatite volcano and the carbonatites of oldoinyo lengai with a review of other occurrences of extrusive carbonatites [PhD Thesis]*, University of London, 1995.
- [53] R. L. Hay, "Natrocarnatite tephra of Kerimasi volcano, Tanzania," *Geology*, vol. 11, no. 10, pp. 599-602, 1983.
- [54] A. N. Mariano and P. L. Roedder, "Kerimasi: a neglected carbonatite volcano," *Journal of Geology*, vol. 91, no. 4, pp. 449-455, 1983.
- [55] J. Žaba and K. Gaidzik, "The Ngorongoro crater as the biggest geotouristic attraction of the Gregory Rift (Northern Tanzania, Africa)-geological heritage," *Geotourism*, vol. 24-25, no. 1, pp. 46-47, 2011.

- [56] A. N. Zaitsev, "Nyerereite from calcite carbonatite at the Kerimasi volcano, northern Tanzania," *Geology of Ore Deposits*, vol. 52, no. 7, pp. 630–640, 2010.
- [57] L. J. McHenry, "Phenocryst composition as a tool for correlating fresh and altered tephra, bed i, Olduvai Gorge, Tanzania," *Stratigraphy*, vol. 2, pp. 101–115, 2005.
- [58] K. Nogami, J. Hirabayashi, Y. Nishimura, and A. Suzuki, "Nature and origin of volcanic ash in the 2000 eruption of Usu volcano, Southwestern Hokkaido," *Japan Earth, Planets and Space*, vol. 54, no. 10, pp. 993–998, 2002.
- [59] D. McLean, P. G. Albert, T. Nakagawa, R. A. Staff, T. Suzuki, and V. C. Smith, "Identification of the Changbaishan 'Millennium' (B-Tm) eruption deposit in the Lake Suigetsu (SG06) sedimentary archive, Japan: synchronisation of hemispheric-wide palaeoclimate archives," *Quaternary Science Reviews*, vol. 150, pp. 301–307, 2016.
- [60] R. Brahm, M. A. Parada, E. Morgado, C. Contreras, and L. E. McGee, "Origin of holocene trachyte lavas of the Quetrupillan volcanic complex, Chile: examples of residual melts in a rejuvenated crystalline mush reservoir," *Journal of Volcanology and Geothermal Research*, vol. 357, pp. 163–176, 2018.
- [61] F. H. Tonneijck, J. van der Plicht, B. Jansen, J. M. Verstraten, and H. Hooghiemstra, "Radiocarbon dating of soil organic matter fractions in andosols in northern Ecuador," *Radiocarbon*, vol. 48, no. 3, pp. 337–353, 2006.